Journal of Geoscience and Environment Protection, 2025, 13(4), 80-96
https://www.scirp.org/journal/gep
ISSN Online: 2327-4344
ISSN Print: 2327-4336

Predictability of Summer (July-September) Extreme Precipitation Days over West Africa during 1982-2022

Yasintha John Forosani[1,2*], Philemon Henry King'uza[1,2], Daniel Stephano Semgomba[1,2]

[1]School of Atmospheric Sciences, Nanjing University of Information Science & Technology, Nanjing, China
[2]Tanzania Meteorological Authority, Dodoma, Tanzania
Email: *fosintaj@gmail.com, ppp3h@outlook.com, semgomba@gmail.com

How to cite this paper: Forosani, Y. J., King'uza, P. H., & Semgomba, D. S. (2025). Predictability of Summer (July-September) Extreme Precipitation Days over West Africa during 1982-2022. *Journal of Geoscience and Environment Protection, 13,* 80-96.
https://doi.org/10.4236/gep.2025.134005

Received: February 26, 2025
Accepted: April 7, 2025
Published: April 10, 2025

Abstract

Extreme precipitation events have substantial socioeconomic effects due to their frequency and intensity. However, predicting and mitigating its effects is difficult due to their influence on society. The present study aims to investigate the predictability of extreme summer precipitation days (EPDs) over West Africa (WA) from 1982 to 2022. Based on daily CHIRPS data spanning 41 years over WA, EPDs were defined using a 90th-percentile threshold at each grid point. A set of Physics-based Empirical (P-E) models is established using the selected predictors. The simultaneous lower boundary anomalies linked to each EPDs index were also analyzed and found that the increased EPDs over WA are accompanied by a Pacific Sea Surface Temperature (SST) impact on monsoon flow and the warming of the SST in the Tropical Atlantic Ocean and western tropical Pacific Ocean. The temporal correlation coefficient (TCC) skill of the cross-validated forecast is 0.80 when the P-E model is constructed using data from 1982 to 2011. The independent forecast determines a significant TCC skill with a 95% level of 0.50 for the remaining period.

Keywords

West Africa, Extreme Precipitation Days, West African Monsoon, Physical Empirical Model, Seasonal Predictability

1. Introduction

Extreme rainfall is considered a double-edged sword, as it can lead to the stagna-

tion of dams and rivers, triggering various floods at global and regional levels (Mubark et al., 2024). Its events are complicated with a high spatiotemporal variation of which its amplification may increase the intensity and frequency of flooding, sometimes accompanied by severe weather such as lightning, hail, strong surface winds, and intense vertical wind shear imposing heavy costs on aquatic and terrestrial ecosystems, human societies, and the economy (Jones et al., 2004; Salack et al., 2018; Tabari, 2020). For example, severe flooding slaughtered more than 800 people in Nigeria, Niger, Chad, and bordering countries between June and October 2022 (carbon brief, 2022) trailed by other shocking floods in 2024 that slaughtered roughly more than 1000 people and displaced hundreds of thousands across the region, particularly in Chad, Nigeria, Mali and Niger, according to the United Nations (UN) (https://apnews.com/article/floods-nigeria-niger-chad-mali-rains-climate-change-397b303cdae17ef2a0076192c8c908ac).

Changes in extreme weather and climate events have significant impacts and are among the most serious challenges to society in dealing with a changing climate (Thomas et al., 2008). Signifying changes in the climatology of extreme rainfall at a regional scale is challenging a monsoon region like WA where heavy rainfall is highly flexible both in space and time thus better attention to the interaction between the coastal upsurge and the monsoon flow could help improve the seasonal predictability of the summer monsoon in WA (De Coëtlogon et al., 2023; Panthou, Vischel, & Lebel, 2014). The reliable predictions on future events of extreme precipitation are crucial for reducing the hazards of these events in WA (Klutse et al., 2024). However, biases in simulating convective systems, shifting climatic teleconnections, and uncertainty in regional processes all have an impact on model reliability. The Guinea Coast region is deliberate to global climatology as its large forest and mangroves could contribute to regulating instabilities and the mechanisms that drive precipitation through global ocean-atmosphere interactions (Ndehedehe et al., 2022). The Ocean regulates extreme precipitation events by acting as a crucial moisture source, affecting the WAM and boosting convective activities with peaks occurring in June to October. The precipitation patterns correspond to the seasonal movement of the ITCZ and are linked to the northward advance of monsoon currents over the land. In West Africa, one of the two low-level westerly regimes important for moisture transport is WAM flow, which is formed by the westward acceleration of the onshore flow across the Guinean Coast (Akinsanola et al., 2015). The impact of these systems on climate zones varies according to the months within the seasonal cycle. The intensified low-level convergence over the warm oceanic region is accompanied by the ascent of moist air, which is subsequently transported by the low-level circulation toward the Guinea Coast (Worou, Fichefet, & Goosse, 2022). The Guinea Coast drives extreme precipitation through moisture convergence and monsoon flow. The West African monsoon (WAM) motivates the seasonal rainfall pattern in WA and displays main southwesterly winds during the summer monsoon months and northeasterlies during the dry season, which is formed by the westward acceleration of

the onto-land flow across the Guinean Coast (Akinsanola et al., 2015; Quagraine et al., 2020). Variations in climate due to instabilities in the tropical oceans, mesoscale convective systems (MCSs), climatic variability indices, and the WAM, topography, SST and the intertropical discontinuity (ITD) significantly influence precipitation patterns which mainly indicate their paths and their intensities (Ebiendele & Adigun 2022; Maurer, Kalthoff, & Gantner, 2017; Vizy & Cook 2022). Skillful prediction of extreme precipitation events would be extremely beneficial to calculate the characteristics of extreme precipitation and their sources to mitigate the increasing threat from a warming climate (Li et al., 2021; Li & Wang, 2018).

Previous studies have shown that rainfall decreases from the Guinea coast to the Sahel subregion (Akinsanola & Zhou, 2020; Ta et al., 2016), with the southern parts of the region receiving high extreme precipitation, whereas areas north of the region show lower values of rainfall extremes. Also, (Akinyoola et al., 2019) added that the increase in precipitation along the Guinea coast due to a rise in the absorption of mineral dust, which in turn raises Single Scattering Albedo, signifies the increase in zonal wind characteristics. Higher precipitation is associated with the seasonal northward migration of the inter-tropical convergence zone (ITCZ), where the subsequent low-level south-westerlies bring moist air inland and converge with the dry north easterly Harmattan winds at the ITD, south of which most rainfall occurs (Berthou et al., 2019; Rodríguez-Fonseca et al., 2015). The changes in precipitation and extremes in WA and Sahel are related to large-scale circulation changes (Diatta et al., 2020). The study of (Klutse et al., 2024), shows that the mean and extreme rainfall are expected to rise in most cities; however, biases in historical models may lead to greater uncertainties in rainfall projection estimations. It revealed that the potential increase in extreme rainfall over WA cities is due to climate changes.

2. Data and Method

2.1. Data

CHIRPS was commonly used in this study for computing the extreme precipitation indices (Diedhiou et al., 2020). Daily CHIRPS data for 41 years from 1982 to 2022 with a spatial resolution of 2.5˚ × 2.5˚ were downloaded and interpolated to 1˚ × 1˚ latitude from https://www.chc.ucsb.edu/monitoring. High spatial resolution and long records make data dependable and suitable for rainfall variability and extremes analysis (Diatta et al., 2020). Mean temperature, SST, Sea Level pressure (SLP), and 850 hPa geopotential height are all downloaded from ERA5. Global Precipitation Climatology Project (GPCP, V2.3) datasets from https://psl.noaa.gov/data/gridded/data.gpcc.html.

2.2. P-E Model

Physically meaningful predictors are chosen, which is the main idea behind creating a P-E model. The initial phase employed lead-lag correlation between the

predictand EPDs and anomalies such as SST, 2-m temperature, and MSLP based on the target months/season to identify areas indicate significant correlation patterns tested at 95% confidence level.

Therefore, here the predictors are expressed by:

$$\text{Pred}(t) = [\text{TF}(t, \text{lat}, \text{lon}) \times \text{TCC}(\text{lat}, \text{lon})], \text{ if } |\text{TCC}(\text{lat}, \text{lon})| > (95\% \text{ confidence level}),$$

where TF denotes the value of a predictor at lead time t and each grid, and TF values at each grid during 1982-2022, and square brackets denote the areal mean over the chosen regions. The purpose of weighing using the temporal correlation coefficient (TCC) is to highlight the shape of the predictors (Zhou et al., 2023). Because of their gradual seasonal fluctuations, we solely reflect the lower border anomalies as predictor fields. Predictors are chosen primarily based on the understanding of the physical linkages between the predictors and predictand (Li & Wang, 2016).

Then, stepwise regression was applied to select the best predictors that fit the model (P-E) construction. The indices that pass the 99% confidence level in stepwise regression were selected for model construction. Additionally, during analysis, more than 14 indices were extracted from different climate parameters and different months/seasons (excluding pointed season) to find out the potential predictors. Two kinds of precursory signals are explored to categorize potential predictors, which are Persistent signals derived from March, April, and May months before the target season and Tendency signals from the short-term tendency of May-June and April-May months from long-term tendency. If the chosen variables show a high correlation, the process will drop to a less significant variable. To dull the overfitting issue, 3 years surrounding an aim year are excluded from the training sample, and the regression model is constructed to predict the aim year. To avoid the artificial preference brought on by the period overlay in predictor selection and verification, all predictors are chosen from the 1982-2012 timeframe, which is the training data for 2012-2022, and a stepwise regression model is constructed. Additionally, the Mean Square Skill Score (MSSS) represents the percentage reduction in the mean square error of the model prediction relative to the climatological forecast, where a positive value indicates superior model performance.

3. Results and Discussion

3.1. EPDs

Regional EPDs were determined if the number of grid points with extreme precipitation on that day was greater than the 90th percentile of entire summer days. For each grid, a daily rainfall measure (daily rainfall > 0.1 mm) is calculated as extreme if it is greater than the threshold. The gridded 90th-percentile value of the series is used as the threshold for extreme daily rainfall to consider the specificity of the precipitation at each grid point (Ta et al., 2016). Because it records extreme precipitation events while excluding moderate ones. This threshold ensures sta-

tistical strength, allows regional climate research, and concentrates on major disasters.

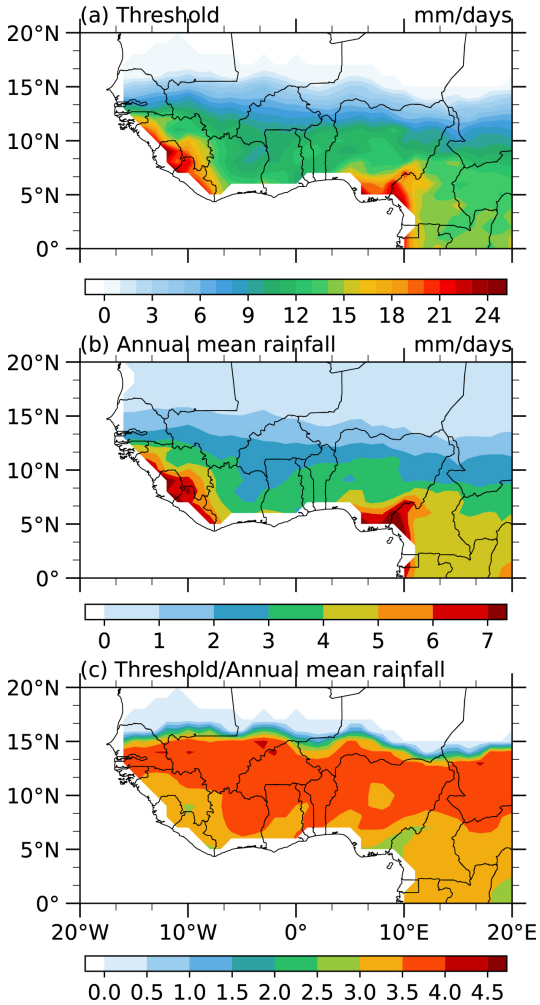

Figure 1. (a) Threshold of extreme precipitation days at the 90th percentile (unit: mm/day), (b) Annual mean precipitation climatology (in mm/day), (c) Ratio of threshold over climatological annual mean precipitation for the period from 1982 to 2022.

Figure 1(a) shows that the threshold decreases from the southern coastal areas near the tropical Atlantic to the northern ones in the Sahelian regions. The rainfall distribution over WA is majorly zonal, with the rainfall decreasing from the coastal to the inland region (Ajibola & Afolayan, 2024). Mostly, it defines areas of high values as, for instance, in the regions 5˚ N - 12˚ N and 4˚ N - 7˚ N, where the maximum is more than 21 mm. **Figure 1(b)** shows that the annual mean rainfall is large in the south coastal areas, reducing towards the Sahelian areas. The threshold and the annual mean rainfall express a similar trend, with the southwest and southeast coastlines of WA receiving maximum precipitation, which happens as the monsoon band advances north; the coast receives more rainfall while the Sahelian regions of the domain receive less. The ratio of threshold to

climatological annual mean precipitation during the whole period around 6˚ N - 15˚ N is practically higher and decreases both sides remarkably in the north (Figure 1(c)).

Figures 2(a)-(c) illustrates the monthly climatological EPDs from July, August to September (JAS) change with the seasons. August month is when significant climatological EPDs values occur frequently, with the region of maximum precipitation shifting northward in accord with the ITD. The North Atlantic ITCZ rainfall belt is positioned around 7˚ N, and rainfall intensities decrease both northward and southward with precipitation peaks along the ITCZ. Substantial rainfall (day precipitation surpassing 50 mm) largely occurs in the southern coastal area of the study area, as shown in Figures 2(d)-(f). The largest center of EPDs appears in August around 10˚N, while the large values of EPDs are in the southern part of WA. The monthly variation of EPDs performed well in the JAS and was reasonably high in August. However, Figure 3 shows the corresponding annual variations of the monthly mean precipitation, implying that JAS may be counted as the summer rainy season for WA. Alike climatological mean precipitation, the monthly EPDs are focused on JAS. This makes it easier to know and forecast the changeability of EPDs across WA. The time series of EPDs-WA is displayed in Figure 4, the demonstrations of the EPDs time series. The related seasonal mean precipitation averaged over WA and the EPDs are seen to show highly consistent year-to-year deviation. The seasonal EPDs and seasonal mean rainfall across WA may have relatively similar sources of predictability. This may indicate that an area-independent extreme precipitation varies in the perspective of global warming.

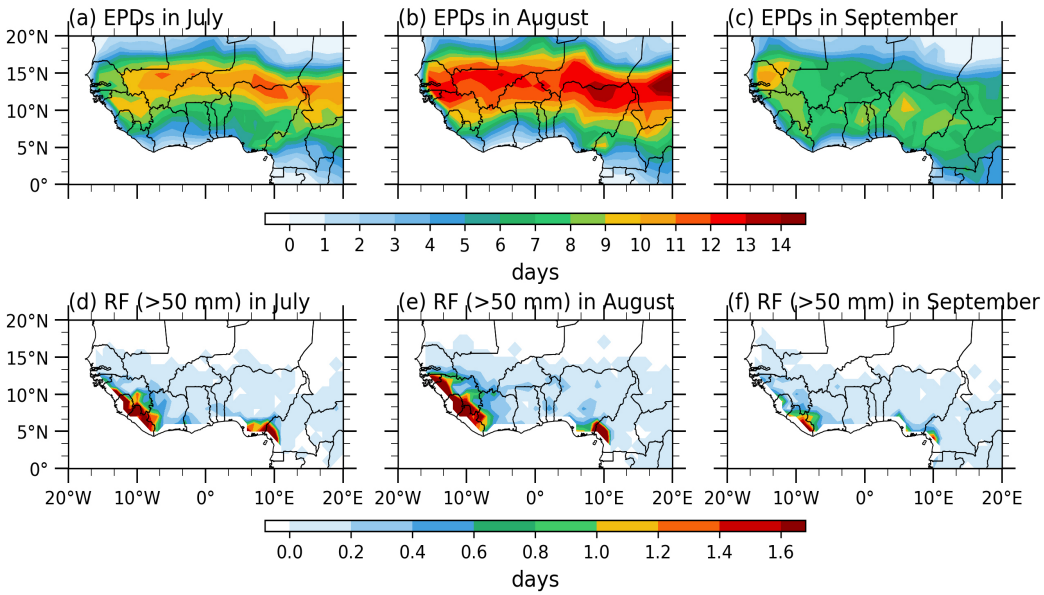

Figure 2. Monthly climatological extreme precipitation days and days with heavy precipitation. Extreme precipitation days (unit: day) during: (a) July, (b) August, and (c) September. Days with heavy precipitation above 50 mm: (d) July, (e) August, and (f) September for the period from 1982 to 2022.

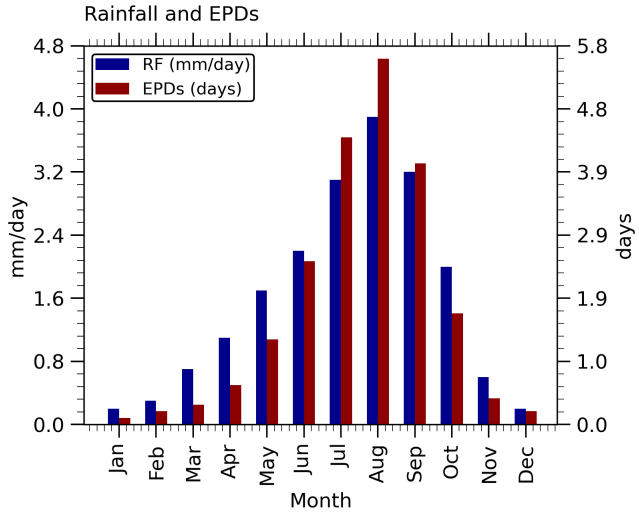

Figure 3. Climatological monthly annual cycle precipitation (blue bar) and monthly extreme precipitation days (red bar) averaged over the West Africa domain at the boundary (20˚ W - 20˚ E, 0˚ - 20˚ N).

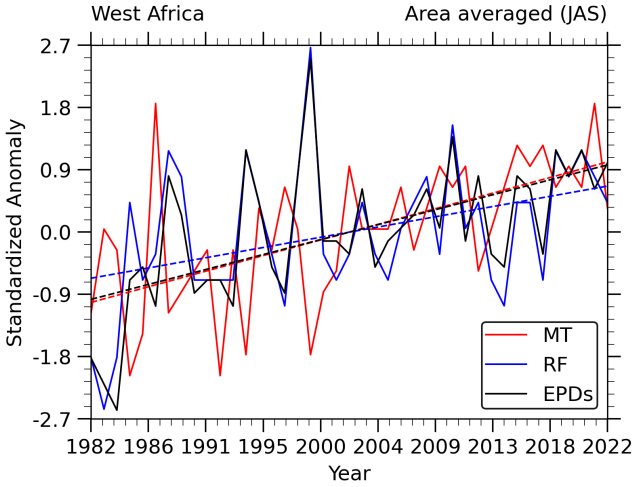

Figure 4. Standardized anomaly annual precipitation (RF, blue line), extreme precipitation days (EPDs, black line), and mean temperature (MT, red line) at two meters, averaged over West Africa domain. Anomaly was computed based on the study period 1982-2022.

3.2. Physical Interpretation of Regional EPDs Indices

Figure 5(a) shows the global distribution of precipitation anomalies during the JAS period, a significant positive correlation between EPDs and precipitation. WA appears to have a notable precipitation anomaly with a large zone of suppressed rainfall near 10˚ N, which shows that the JAS rainfall anomaly in WA is more closely linked to EPDs. Figure 5(b) displays the mean sea level pressure (MSLP) and wind anomalies at 850 hPa. The intensity of equatorial westerlies and the Saharan easterlies are clearly observed in the 850 hPa. The wind vectors in the tropics are important as they reflect the strength and direction of the trade winds,

which influence moisture transport and WAM. The westerlies over the Atlantic Ocean bring moisture to the region. Negative pressure anomalies, particularly over the tropical Atlantic, enhance the land-ocean pressure gradient, intensifying southwesterly monsoon winds and moisture transport, thereby strengthening convection and increasing extreme rainfall over WA during JAS. Figure 5(c) shows the temperature anomalies at 2 meters above the surface (2 mT) and SST,

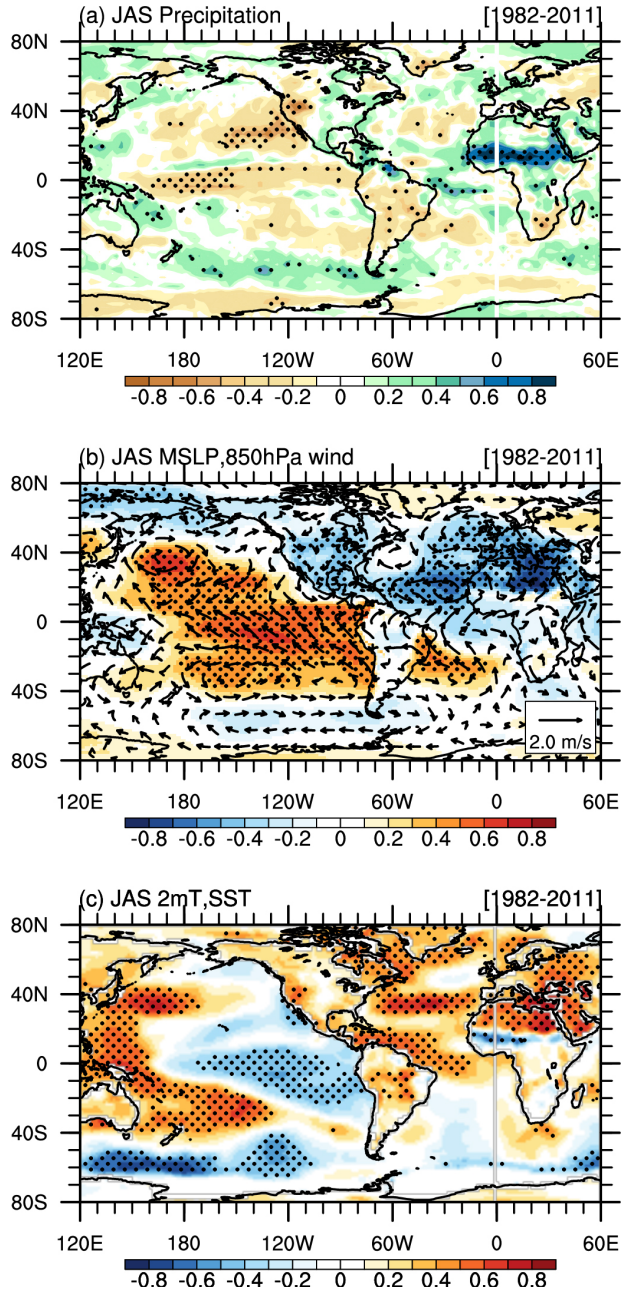

Figure 5. Spatial correlation between extreme precipitation days (EPDs) and atmospheric and oceanic variables in July-August-September from 1982 to 2011. (a) Precipitation, (b) Mean Sea level pressure (shading), and wind vectors at 850 hPa. (c) Sea surface temperature and two-meter air temperature over the continent. Areas with black dots indicate correlation values significant at a 95% confidence level.

the tropical Atlantic and parts of the western pacific have significantly warm SSTs which could be linked with the increased EPDs in the region since the warming up in these oceanic regions is associated with an intensification of extreme precipitation events. A thermal low-pressure system over the Sahara Desert attains maximum intensity in summer, increasing the meridional temperature differential and generating a greater pressure differential between the Gulf of Guinea and the Sahara, which is linked to WAM, which leads to significant inland moisture penetration and improved representation of ITCZ rainfall.

Figure 6(a) shows the warm Pacific SST anomalies from March to September contribute to increased EPDs during the time with a peak from June to September. The warm tropical Atlantic SST anomalies from May to September are associated with a higher frequency of EPDs in WA, particularly during July to September when WAM is most active (**Figure 6(b)**). A strong correlation between precipitation and oceanic regions along the African monsoon route significantly improves seasonal rainfall forecasts in the region (Hamatan et al., 2004; Hounkpè et al., 2021).

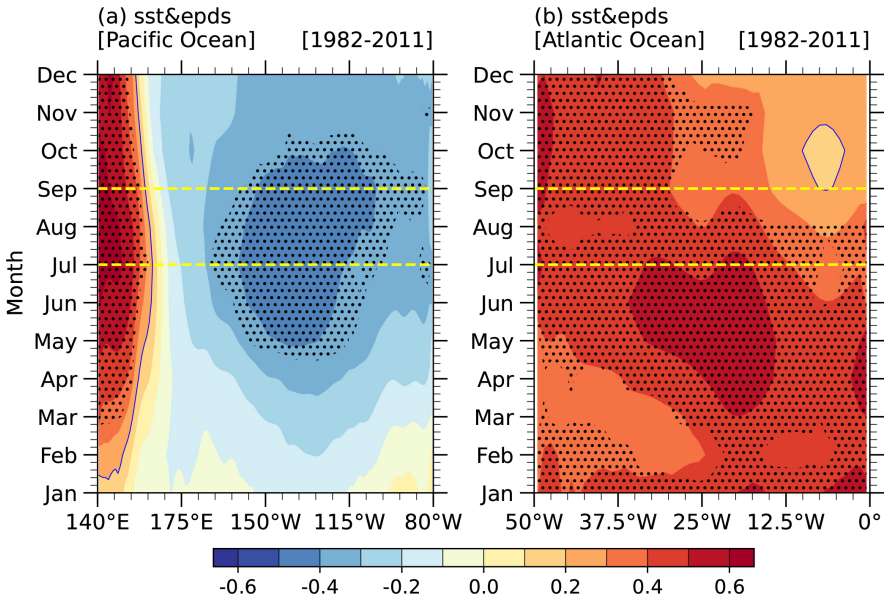

Figure 6. Zonal cross-section correlation between sea surface temperature (SST) averaged over 5˚ S - 5˚ N reshaped in monthly and extreme precipitation days during 1982-2011. (a) Pacific Ocean and (b) Atlantic Ocean. Areas with black dots indicate correlation values significant at a 95% confidence level.

For EPDs-WA, three predictors are chosen. The first predictor, which features the SST anomalies during MAM, is correlated to EPDs. The positive correlations in the north Africa and western parts of the Pacific Ocean are linked to extreme precipitation. Negative correlations seen in the southeastern Pacific imply that cooler SSTs in this region correspond with more extreme precipitation in this region (**Figure 7(a)**). The warming in the western Pacific and cooling in the central and southeastern regions enhance WAM in ensuing JAS (**Figure 8(c)**) through

atmospheric circulation (Figure 8(b)). The associated westerlies transport warm moisture into WA foremost to deepen precipitation over the region (Figure 8(a)-(b)).

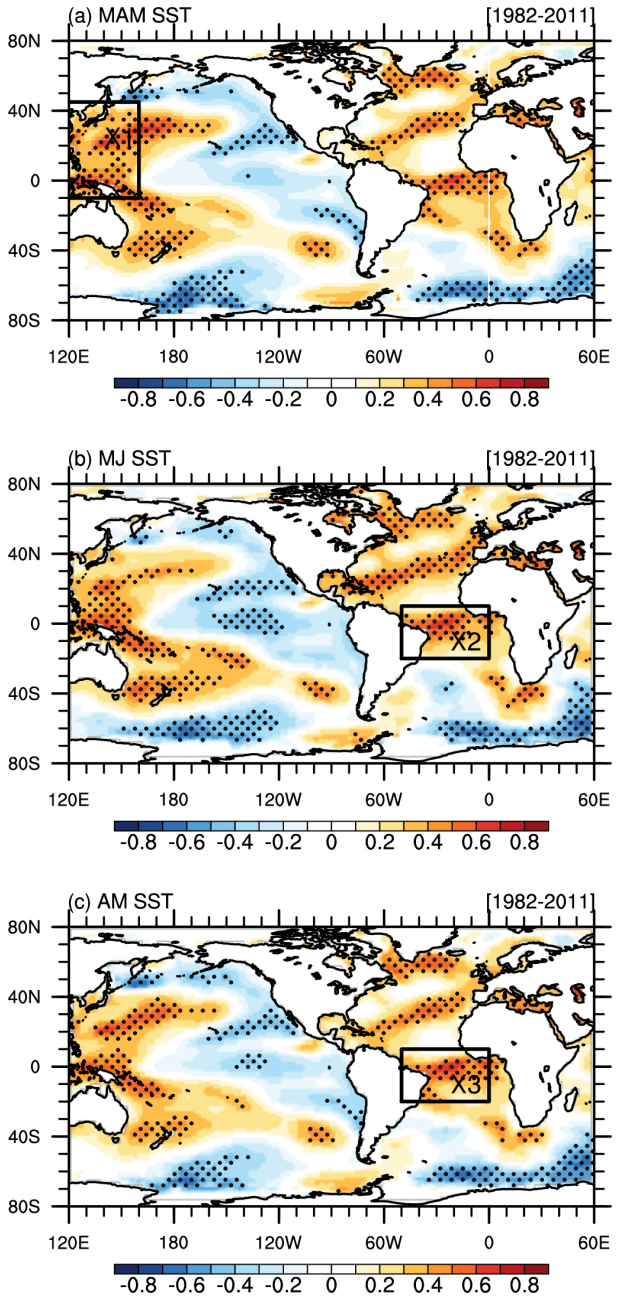

Figure 7. Correlation map between extreme precipitation days and (a) Sea surface temperature (SST) during March-April-May mean, (b) SST during May-June mean and (c) SST during April-May mean, from 1982 to 2011. The regions indicated by black boxes show the location of predictors X1 (120˚ - 160˚ E, 10˚ S - 45˚ N), X2 (0˚ - 50˚ W, 20˚ S-10˚ N) and X3 (0˚ - 50˚ W, 25˚ S - 10˚ N). Areas with black dots indicate correlation values significant at a 95% confidence level.

The second and third predictors feature high SST anomalies over the tropical

Atlantic during MJ and AM, respectively (**Figure 7(b)**, **Figure 7(c)**). The high SST anomalies cause anomalous warming in the Atlantic Ocean and convergence over WA through ocean-land interaction (**Figure 9(c)**, **Figure 10(c)**). The trade wind transferred the warm moisture to WA and hence increased extreme precipitation over the region (**Figure 9(a)**, **Figure 10(a)**, **Figure 9(b)**, **Figure 10(b)**). The low-level southwesterly monsoon flow at around 850 hPa is the key driver of moisture from the Atlantic Ocean to the continent (Akinsanola & Zhou, 2020).

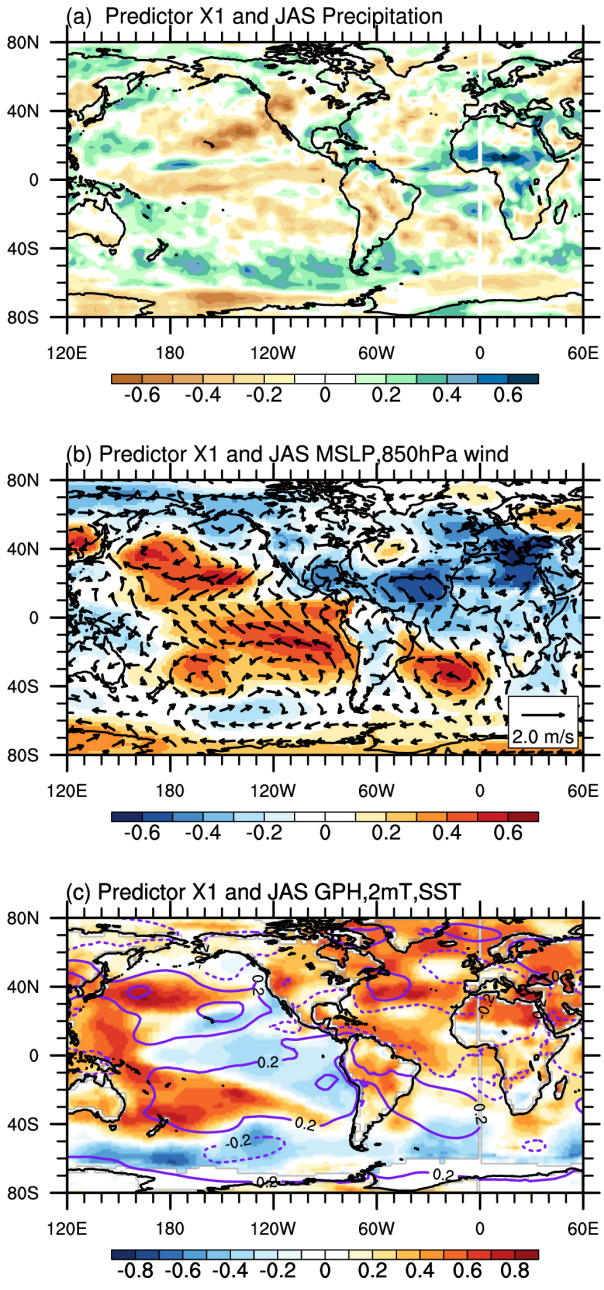

Figure 8. Correlation map between predictor X1 and March-April-May mean (a) Precipitation, (b) Mean Sea level pressure (shading) and wind vectors at 850 hPa, and (c) Geopotential height (contour line), sea surface temperature (over Oceans) and two-meter air temperature (over the continent) during 1982-2011.

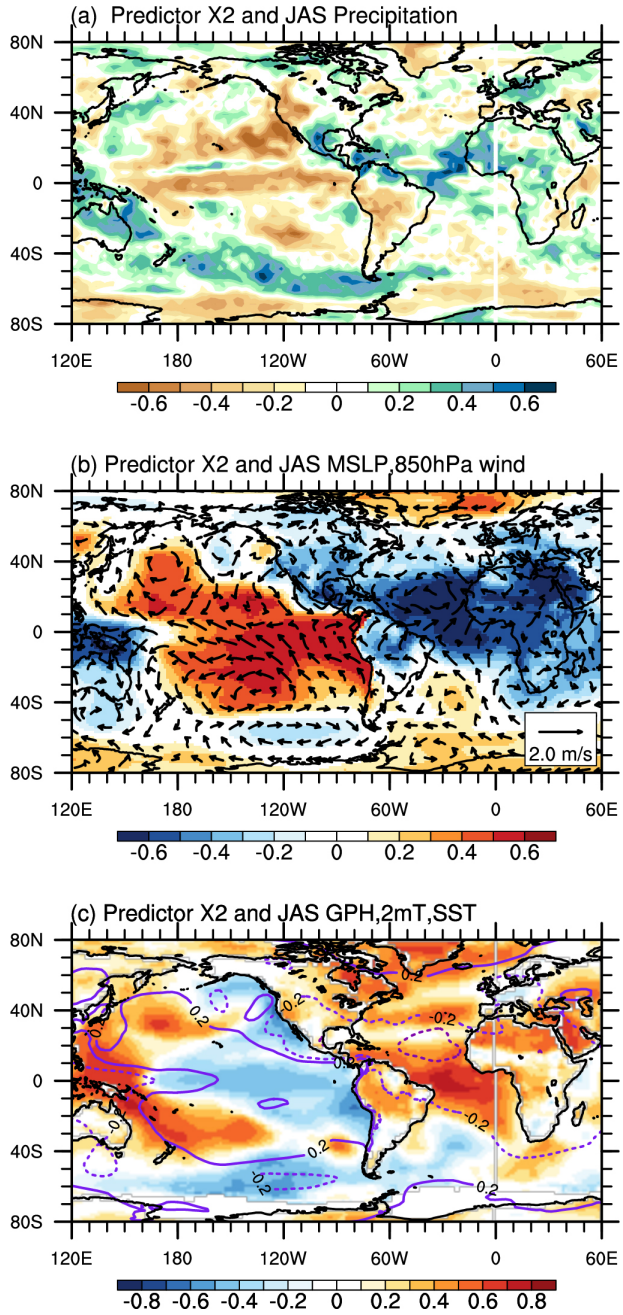

Figure 9. Correlation map between predictor X2 and May-June mean (a) Precipitation, (b) Mean Sea level pressure (shading) and wind vectors at 850 hPa, and (c) Geopotential height (contour line), sea surface temperature (over Oceans) and two-metre air temperature (over the continent) during 1982-2011.

3.3. Predictability of EPDs over WA

A series of stepwise regression equations were constructed for each EPD indicator based on physical predictors. As displayed in **Figure 11**, the cross-validated re-forecast and independent forecast EPDs indices generated by the P-E models effectively capture the interannual variation of observed EPDs indices, representing that the P-E models hold strong predictive capability for EPDs in the region of

WA. For EPDs-WA, the TCC (MSSS) skill of the cross-validated forecast is 0.80 (0.57) when the P-E model is constructed using data from 1982 to 2011, the independent forecast demonstrates significant TCC skill with a 95% level) of 0.50 (0.24) for the following decade (2012-2022). Table 1 shows that three predictors of EPDs over WA are independent of each other, which increases the accuracy of the prediction.

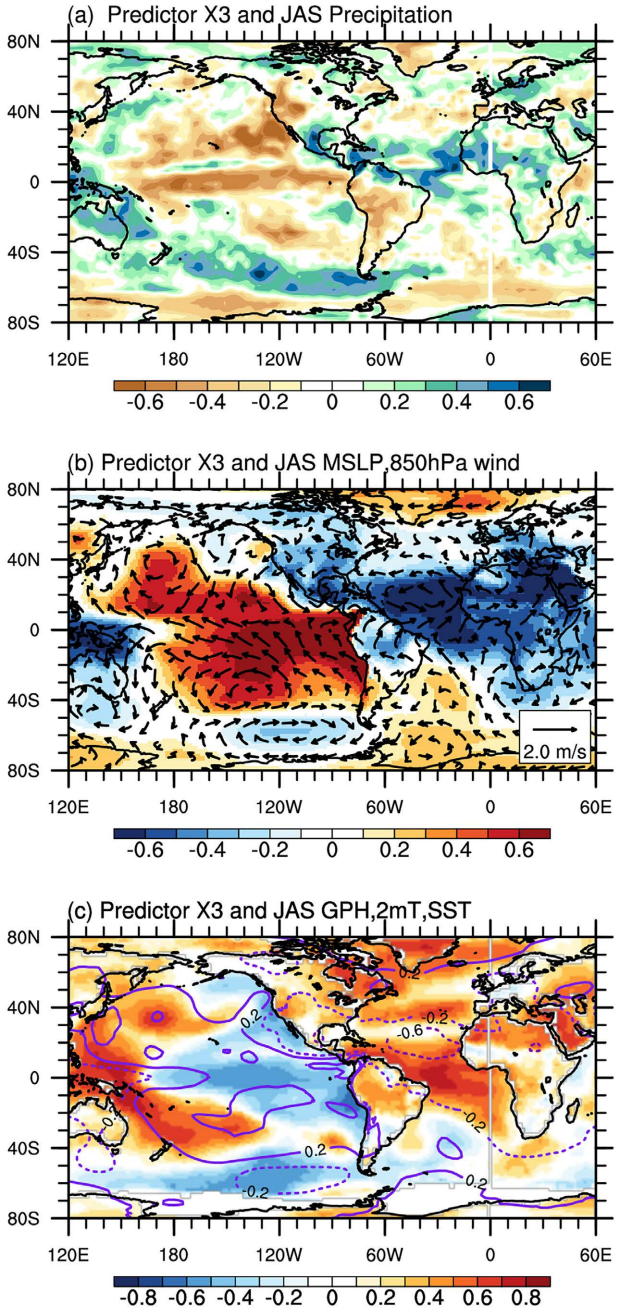

Figure 10. Correlation map between predictor X3 and April-May mean (a) Precipitation, (b) Mean Sea level pressure (shading) and wind vectors at 850 hPa, and (c) Geopotential height (contour line), sea surface temperature (over Oceans) and two-meter air temperature (over the continent) during 1982-2011.

Table 1. The temporal correlation coefficient between EPDs and individual predictors (indices) from 1982 to 2011.

Indices	X1	X2	X3
TCC	0.71	0.55	0.50
p-value	1.24E-5	0.0018	0.0051

Note: All correlation values are significant at a 99% confidence level (*p*-values < 0.01).

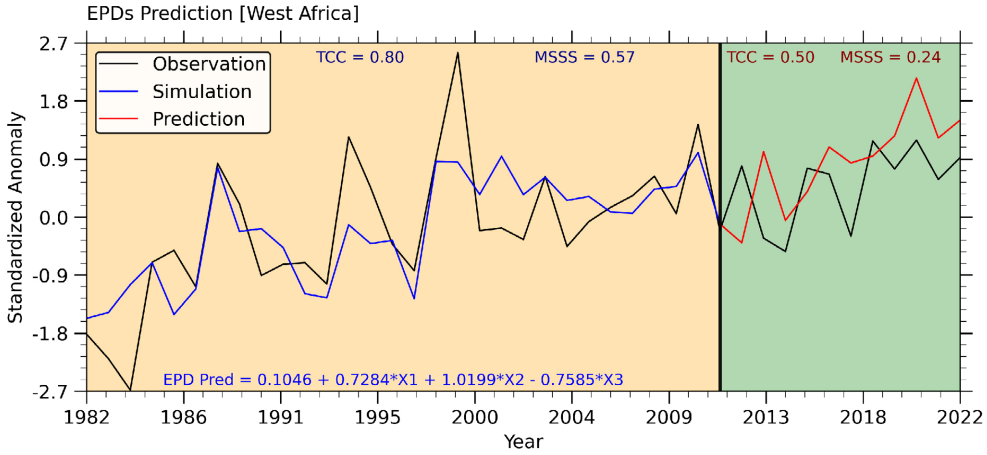

Figure 11. Time series of extreme precipitation days (EPDs, black line) during 1982-2022, simulated EPDs (blue line) during 1982-2011, and forecasted EPDs (red line) during 2011-2022.

4. Summary

These findings intend to increase predictions of summer EPDs over WA:

I) The correlations between SST anomalies in the equatorial Atlantic and precipitation over the Gulf of Guinea are prevailing appearances. The SST shows positive significant values, suggesting that anomalous warming in the Atlantic Ocean between 40˚ W and 0˚ W is linked to both a strengthening of the anticyclone of Saint Helena and an increase in extreme precipitation events to the WA. Ocean atmosphere dynamics can boost the prediction of extreme rainfall events in WA.

II) Summer extreme precipitation thresholds and mean rainfall marked a definite decreasing trend from the south coast to northern WA, emphasizing significant regional variability. This is because, as a coastal region, the south of WA is influenced by the monsoon and evaporation at the Atlantic Ocean's level, which are known to be the rainiest areas and to have the longest rainy season in WA (Ta et al., 2016; Tore et al., 2022).

III) A strong correlation between summer EPDs and mean rainfall demonstrates comparable backgrounds and predictability sources, which means the prediction skill for EPDs is substantially determined by the ability to predict summer mean rainfall.

IV) The low SLP anomalies in the equatorial Atlantic and dipolar SST anomalies contribute to atmospheric circulation and influence the existence of extreme precipitation events in WA. Significant negative SLP anomalies in the equatorial

Atlantic enhance moisture convergence over WA.

V) The cross-validated forecast (independent forecast) of EPDs for 1982-2012 (2012-2022) accomplishes a substantial TCC skill of 0.80 (0.50) for WA. These excellent skills derived from the P-E models suggest an assessment of the lower bound of predictability for summer EPDs over WA for the present forecast year.

VI) La Nina increases the monsoon flow and increases EPDs over WA. The study of (Mohino et al., 2023) backed up by stating that the Pacific SST effect shows a large impact in the monsoon season and after the monsoon withdrawal, unlike the Indian SST effect.

The study is fundamental for understanding extreme weather occurrences and their prediction. This information can facilitate the development of early warning systems, educate people about the sources of predictability of EPDs over WA, and address the lack of WA-specific climate research. This information will enable authorities to plan for probable floods and other meteorological disasters, advising decision-makers on appropriate mitigation and adaptation measures for extreme climate events. We encourage developing adaptation and mitigation methods based on geography, as extreme rainfall occurrences vary greatly throughout geographies.

Conflicts of Interest

The authors declare no conflicts of interest regarding the publication of this paper.

References

Ajibola, F. O., & Afolayan, S. A. (2024). Impacts of Improved Horizontal Resolutions in the Simulations of Mean and Extreme Precipitation Using CMIP6 HighResMIP Models over West Africa. *Environmental Monitoring and Assessment, 196,* Article No. 328. https://doi.org/10.1007/s10661-024-12492-7

Akinsanola, A. A., & Zhou, W. (2020). Understanding the Variability of West African Summer Monsoon Rainfall: Contrasting Tropospheric Features and Monsoon Index. *Atmosphere, 11,* Article 309. https://doi.org/10.3390/atmos11030309

Akinsanola, A. A., Ogunjobi, K. O., Gbode, I. E., & Ajayi, V. O. (2015). Assessing the Capabilities of Three Regional Climate Models over CORDEX Africa in Simulating West African Summer Monsoon Precipitation. *Advances in Meteorology, 2015,* Article ID: 935431. https://doi.org/10.1155/2015/935431

Akinyoola, J. A., Ajayi, V. O., Abiodun, B. J., Ogunjobi, K. O., Gbode, I. E., & Ogungbenro, S. B. (2019). Dynamic Response of Monsoon Precipitation to Mineral Dust Radiative Forcing in the West Africa Region. *Modeling Earth Systems and Environment, 5,* 1201-1214. https://doi.org/10.1007/s40808-019-00620-z

Berthou, S., Kendon, E. J., Rowell, D. P., Roberts, M. J., Tucker, S., & Stratton, R. A. (2019). Larger Future Intensification of Rainfall in the West African Sahel in a Convection-Permitting Model. *Geophysical Research Letters, 46,* 13299-13307. https://doi.org/10.1029/2019gl083544

de Coëtlogon, G., Deroubaix, A., Flamant, C., Menut, L., & Gaetani, M. (2023). Impact of the Guinea Coast Upwelling on Atmospheric Dynamics, Precipitation and Pollutant Transport over Southern West Africa. *Atmospheric Chemistry and Physics, 23,* 15507-15521. https://doi.org/10.5194/acp-23-15507-2023

Diatta, S., Diedhiou, C. W., Dione, D. M., & Sambou, S. (2020). Spatial Variation and Trend of Extreme Precipitation in West Africa and Teleconnections with Remote Indices. *Atmosphere, 11,* Article 999. https://doi.org/10.3390/atmos11090999

Diedhiou, C. W., Diatta, S., Ndione, D. M., & Sambou, S. (2020). Spatial Variation and Trend of Extreme Precipitation in West Africa and Teleconnections with Remote Indices. *Atmosphere, 11,* Article 999.

Ebiendele, P. E., & Adigun, P. A. (2022). *Added Value of Bias Adjusted and Statistical Downscaled ISIMIP Models in Simulating Extreme Precipitation Characteristics over West Africa* (pp. 1-28). https://www.researchsquare.com/article/rs-2028519/v1

Hamatan, M., Mahe, G., Servat, É., Paturel, J. E., & Amani, A. (2004). Synthèse et Évaluation Des Prévisions Saisonnières En Afrique de l'Ouest. *Sécheresse, 15,* 279-286.

Hounkpè, J., Badou, D. F., Bossa, A. Y., Yira, Y., Adounkpè, J., Alamou, E. A. et al. (2021). Assessment of Flood Discharge Sensitivity to Climate Indexes in West Africa. *Proceedings of the International Association of Hydrological Sciences, 384,* 219-224. https://doi.org/10.5194/piahs-384-219-2021

Jones, C., Waliser, D. E., Lau, K. M., & Stern, W. (2004). Global Occurrences of Extreme Precipitation and the Madden-Julian Oscillation: Observations and Predictability. *Journal of Climate, 17,* 4575-4589. https://doi.org/10.1175/3238.1

Klutse, N. A. B., Abiodun, B. J., Quagraine, K. A., Nkrumah, F., Abaton, A. A., Adekoke, J. et al. (2024). Projected Changes in Rainfall Extremes over West African Cities under Specific Global Warming Levels Using CORDEX and NEX-GDDP Datasets. *Earth Systems and Environment, 8,* 747-764. https://doi.org/10.1007/s41748-024-00425-w

Li, J., & Wang, B. (2016). How Predictable Is the Anomaly Pattern of the Indian Summer Rainfall? *Climate Dynamics, 46,* 2847-2861. https://doi.org/10.1007/s00382-015-2735-6

Li, J., & Wang, B. (2018). Predictability of Summer Extreme Precipitation Days over Eastern China. *Climate Dynamics, 51,* 4543-4554. https://doi.org/10.1007/s00382-017-3848-x

Li, J., Qian, Y., Leung, L. R., & Feng, Z. (2021). Summer Mean and Extreme Precipitation over the Mid-Atlantic Region: Climatological Characteristics and Contributions from Different Precipitation Types. *Journal of Geophysical Research: Atmospheres, 126,* e2021JD035045. https://doi.org/10.1029/2021jd035045

Maurer, V., Kalthoff, N., & Gantner, L. (2017). Predictability of Convective Precipitation for West Africa: Verification of Convection-Permitting and Global Ensemble Simulations. *Meteorologische Zeitschrift, 26,* 93-110. https://doi.org/10.1127/metz/2016/0728

Mohino, E., Monerie, P. A., Mignot, J., Diakhaté, M., Donat, M., Roberts, C. D., & Doblas-Reyes, F. (2023). *Impact of AMV on Rainfall Intensity Distribution and Timing of the West African Monsoon in DCPP-C-Like Simulations.*

Mubark, A., Chen, Q., Abdallah, M., Hussien, A., & Hamadalnel, M. (2024). Projection of Extreme Summer Precipitation over Hubei Province in the 21st Century. *Atmosphere, 15,* Article 983. https://doi.org/10.3390/atmos15080983

Ndehedehe, C. E., Usman, M., Okwuashi, O., & Ferreira, V. G. (2022). Modelling Impacts of Climate Change on Coastal West African Rainfall. *Modeling Earth Systems and Environment, 8,* 3325-3340. https://doi.org/10.1007/s40808-021-01302-5

Panthou, G., Vischel, T., & Lebel, T. (2014). Recent Trends in the Regime of Extreme Rainfall in the Central Sahel. *International Journal of Climatology, 34,* 3998-4006. https://doi.org/10.1002/joc.3984

Quagraine, K. A., Nkrumah, F., Klein, C., Klutse, N. A. B., & Quagraine, K. T. (2020). West

African Summer Monsoon Precipitation Variability as Represented by Reanalysis Datasets. *Climate, 8,* Article 111. https://doi.org/10.3390/cli8100111

Rodríguez-Fonseca, B., Mohino, E., Mechoso, C. R., Caminade, C., Biasutti, M., Gaetani, M. et al. (2015). Variability and Predictability of West African Droughts: A Review on the Role of Sea Surface Temperature Anomalies. *Journal of Climate, 28,* 4034-4060. https://doi.org/10.1175/jcli-d-14-00130.1

Salack, S., Saley, I. A., Lawson, N. Z., Zabré, I., & Daku, E. K. (2018). Scales for Rating Heavy Rainfall Events in the West African Sahel. *Weather and Climate Extremes, 21,* 36-42. https://doi.org/10.1016/j.wace.2018.05.004

Ta, S., Kouadio, K. Y., Ali, K. E., Toualy, E., Aman, A., & Yoroba, F. (2016). West Africa Extreme Rainfall Events and Large-Scale Ocean Surface and Atmospheric Conditions in the Tropical Atlantic. *Advances in Meteorology, 2016,* Article ID: 1940456. https://doi.org/10.1155/2016/1940456

Tabari, H. (2020). Climate Change Impact on Flood and Extreme Precipitation Increases with Water Availability. *Scientific Reports, 10,* Article No. 13768. https://doi.org/10.1038/s41598-020-70816-2

Thomas, R. K., Gerald, A. M., Christopher, D. M., & William, L. M. (2008). *Weather and Climate Extremes in a Changing Climate Regions of Focus.* https://www.sdr.gov/pdfs/Presentations/CCSP_SAP3_3_WeatherAndClimateExtremesInAChangingClimate.pdf

Tore, D. B., Alamou, A. E., Obada, E., Biao, E. I., & Zandagba, E. B. J. (2022). Assessment of Intra-Seasonal Variability and Trends of Precipitations in a Climate Change Framework in West Africa. *Atmospheric and Climate Sciences, 12,* 150-171. https://doi.org/10.4236/acs.2022.121011

Vizy, E. K., & Cook, K. H. (2022). Distribution of Extreme Rainfall Events and Their Environmental Controls in the West African Sahel and Soudan. *Climate Dynamics, 59,* 997-1026. https://doi.org/10.1007/s00382-022-06171-x

Worou, K., Fichefet, T., & Goosse, H. (2022). Future Changes in the Mean and Variability of Extreme Rainfall Indices over the Guinea Coast and Role of the Atlantic Equatorial Mode. *Weather and Climate Dynamics, 4,* 511-530.

Zhou, Z., Li, J., Chen, H., & Zhu, Z. (2023). Seasonal Prediction of Extreme High-Temperature Days in Southwestern China Based on the Physical Precursors. *Advances in Atmospheric Sciences, 40,* 1212-1224. https://doi.org/10.1007/s00376-022-2075-5